RESPONSE OF THE FSSP-100 AND PVM-100A TO SMALL ICE CRYSTALS

Hermann Gerber*
Gerber Scientific, Inc., Reston, VA

P.J. DeMott
Colorado State University, Ft. Collins, CO 80523

1. INTRODUCTION

Ambient ice crystals smaller than about 50- m diameter can contribute significantly to ice water content (IWC) in cirrus clouds, especially near cloud top and at cold temperatures (Heymsfield and Miloshevich, 2003; Heymsfield et al., 2010). The crystal measurements with forward-scattering probes that are sensitive to this size range such as the FSSP-100 (formerly from Particle Measuring Sysystems, Inc.), the CPD and CAS (from Particle Measurement Technologies), and the PVM-100A (from Gerber Scientific, Inc.) have potential problems as noted by Baumgardner et al. (2011) and Wendisch and Brenguier (2013). These probes are designed to measure spherical particles; whereas, ice crystals are usually aspheric causing errors in the desired ice-crystal properties. A second problem has been the potential shattering of the crystals on the inlets of the probes causing spurious concentrations of small crystals. This latter problem has been addressed by Korolev et al. (2011, 2013) who showed that redesign of the probes' inlet geometries reduced significantly the shattering effect. Given this improvement, the present study takes another look at the performance of forward-scattering probes since their measurements of small ambient ice crystals may now be more useful.

This study has two parts. The 1st describes meaurements with two of the probes, FSSP-100 and PVM-100A in the Colorado State University Dynamic Cloud Chamber (DCC; DeMott, 1988, 1990; DeMott and Rogers, 1990) of small ice crystals generated therein (Gerber etal., 1995). The 2nd part calculates a correction factor applicable to the two probes for their measurements of ice-crystal IWC and effective radius (Re). The correction factor (C_f) is based on ice crystal habits including randomly-oriented plates, columns, dendrites, and rosettes described by Takano and Liou (1995). Finally, the application of C_f to the FSSP and PVM chamber measurements is compared to reference values determined for the ice crystals generated in the DDC. This study is fully described in Gerber and DeMott (2014; AMS copyright); figures 1–5 are reproduced from this paper.

2. DCC CHAMBER MEASUREMENTS

2.1 *Instrumentation*

The DCC consists of an insulated 1.2-m^3 thermally-controlled copper cloud chamber which can be cooled to match adiabatic cooling during expansion. Vents and windows in the DCC provide access for probes and aerosol and gas injection. The range of operation of the chamber for temperature is +40 ^{0}C to -55 ^{0}C, is 90 kpa to 50 kpa for pressure, is 0.1% to >100% for RH, and is 0.2 m s^{-1} to 20 m s^{-1} for simulated vertical velocity. Dew-point hygrometers monitor RH, and thermocouples measure inside-air and chamber wall temperature. A 1-D probe (230-X) and the FSSP draw air out of the camber for their measurements. The PVM is located inside the chamber. A video microscope consists of a continuously moving 16-mm film loop which passes out of the chamber and under a microscope that generates CCD images for a video recorder. Images of ice crystals sedimented on the film loop are manually evaluated for size and habit.

2.2 *Measurements*

The procedure used to generate ice crystals in the DCC is to moisten and seed the chamber with CCN, to cool and lower the pressure in the chamber until a cloud forms, and to keep cooling until a desired temperature is reached when IN (ice nuclei) are injected and ice nucleation occurs. Figure 1 is an example of one of the 18 ice-crystal runs made in the DCC showing time dependence of temperature, moisture, and FSSP and 230-X outputs. The crystal habits generated during the experiments included mostly hexagonal columns and plates, some plates with dendritic features, and some spherical poly-crystals. In most of the experiments the crystals were within the known size range of the FSSP.

Figure 2 shows details of IWC, PSA (Particle Surface Area), and FSSP and 230-X measurements for Experiment 18 where crystals were predominantly small columns. The top plots compare the uncorrected IWC measure (PVMWC) by the PVM with the reference IWC (TOTWC) determined from manual evaluation of the crystals on the film loop (over the intervals I14 and I15) and from the application of the Redder and Fukuta (1989) algorithm that relates crystal size and shape to crystal mass. The comparison shows that the PVM over-estimates IWC in comparison to the reference, because the PVM is calibrated for spherical particles. The middle plots compare PSA in a similar manner. Here agreement is good between PSA measured by the PVM and the reference, because the PVM should measure accurately the ice crystals projected area since it measures a small angular range of near-forward scattered diffracted light from the crystals. The FSSP may also measure PSA properly; although, its angular measurement range is larger. The bottom plots show the crystal size spectra measured by the FSSP and 230-X.

* Corresponding author address: H. Gerber, Gerber Scientific, Inc., Reston, VA 20190; email: hgerber6@comcast.net

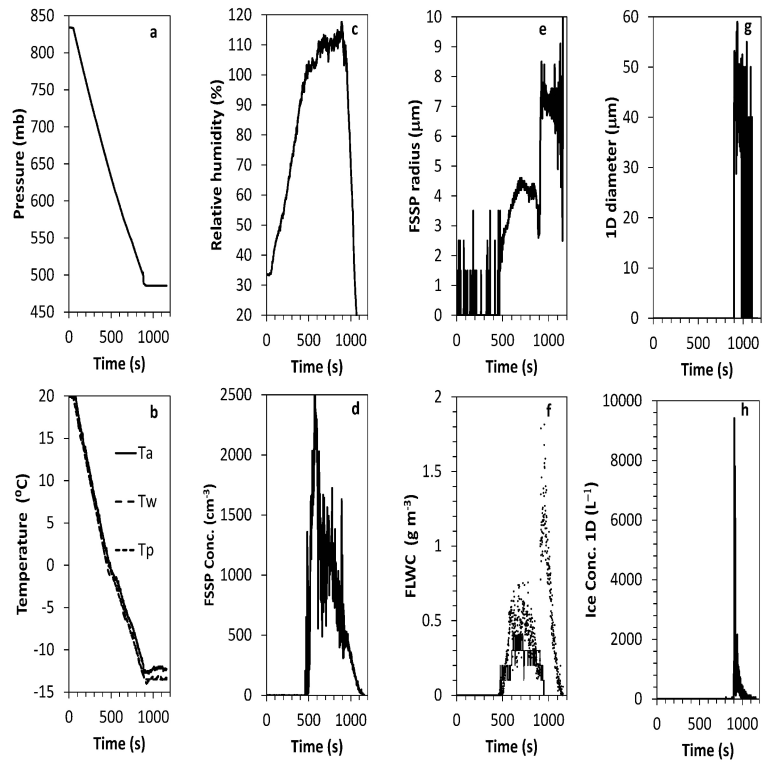

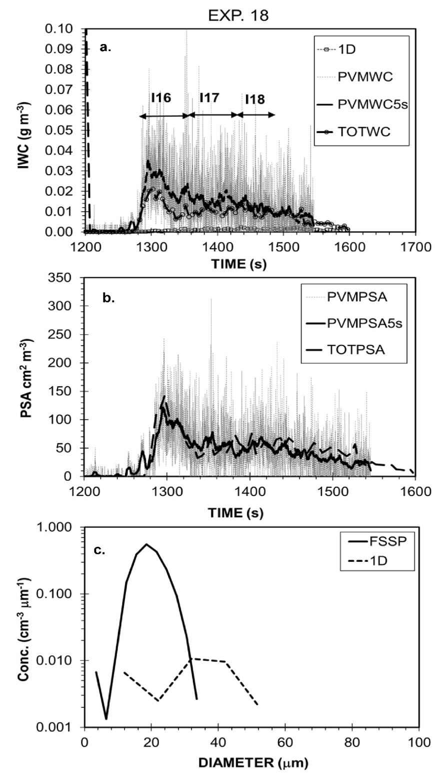

Fig. 1 - Pressure (a), temperature (b; Ta = air, Tw = wall, Tp = program), and humidity (c) in the CSU Dynamic Cloud Chamber (DCC), and FSSP (d,e,f) and 230-X (1-D, g,h) data as a function of time during the run of Experiment 5. FSSP data in (f) is the water and ice mass concentration (dots); line data in (f) is water concentration measured by the heated hygrometer. The supercooled water cloud glaciates at time ~ 920 s.

Fig. 2 - a. Comparison of 1-hz and 5-s average PVM IWC data for Exp. 18 to reference TOTWC for small hexagonal ice crystals. b. Comparison of PSA to reference TOTPSA. c. Mean FSSP and 1-D spectra.

3. IWC AND EFFECTIVE RADIUS CORRECTION FACTORS

Much has been written on parameterizing the output of ice-crystal probes to determine IWC, PSA, effective density and other parameters of ice crystals. The most popular procedure for doing this is to utilize a circle circumscribed around ice-crystal images obtained from imaging probes. Here a different approach is used which takes advantage that both the FSSP, PVM and other forward-scattering probes are thought to measure predominantly diffracted light scattered by the crystals. The diffracted light should be proportional to the projected area, G, of aspheric particles (Van De Hulst, 1962) which includes ice crystals. Applying the assumption that the crystals are randomly oriented in space yields G = PSA/4 (Takano and Liou, 1995).

It can be shown (Gerber and DeMott, 2014) that ice volume V_d , as measured by the FSSP and PVM of an aspheric ice crystal, is related to G:

$$V_d = 4\,\pi^{-1/2}\,G^{3/2} / 3$$

which is termed the *diffraction volume*. This volume is larger than the actual volume V of the ice crystal so that a correction factor can be defined as

$$C_f = \frac{V}{V_d} \quad .$$

Using the above two equations and the equations for IWC and PSA for spherical ice crystals results in

$$IWC = \rho_i V_d C_f$$

and

$$\mathrm{Re} = \frac{3 V_d C_f}{4 G} .$$

for aspheric ice crystals given that C_f is known.

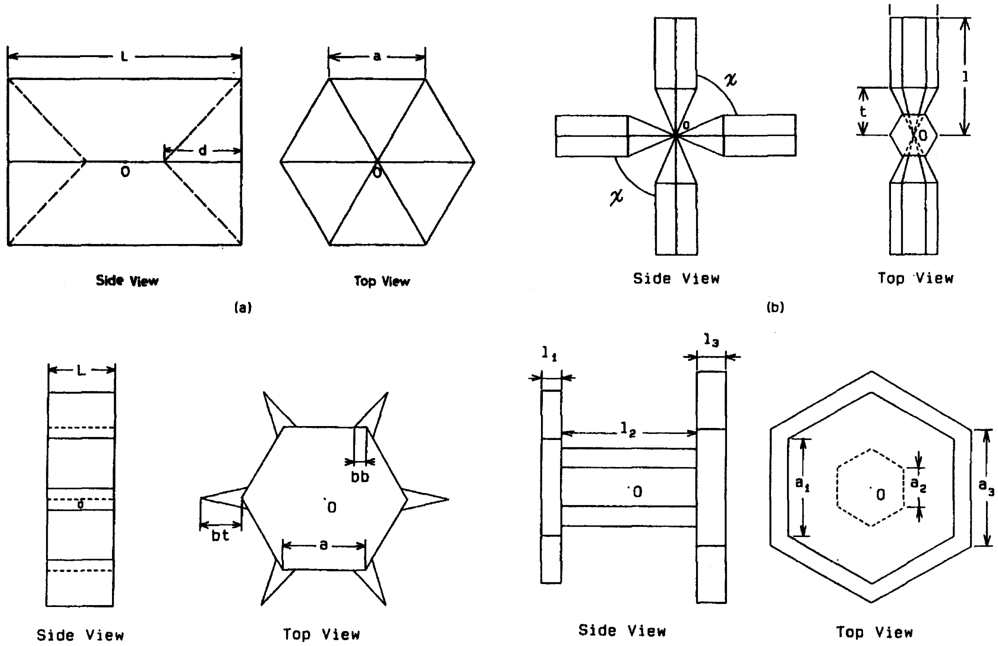

Fig. 3 - Model geometry for (a) hollow column, (b) bullet rosette, (c) dendrite, and (d) capped column (reproduced with permission from Takan and Liou 1995).The lengths, L and l, in this plot are changed to the symbol c in the present analysis, and the width 2a of the crystals remains the same. bb is the dendrite branch width and bt is its length. The mean crossing angle between the arms of the bullet rosette.

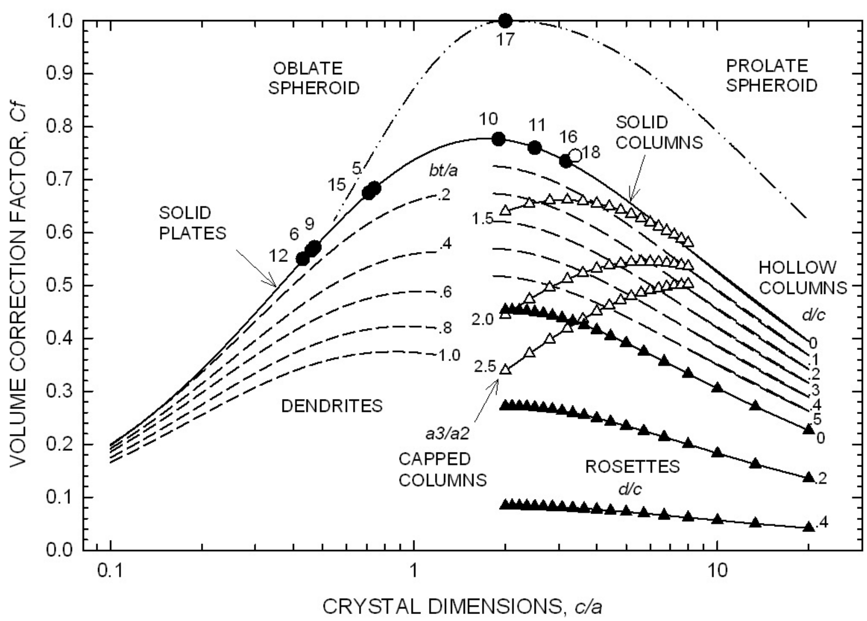

Fig. 4 - Ice crystal volume correction factor C_f for the ice-crystal habits shown in Fig. 3 and for spheroids as a function of ice-crystal dimensions where c is the crystal length (or thickness) and a is ½ the crystal width. The numbered circles data refer to results from the crystal measurements for different experiments in the DCC. The spheroid results are based on a publication by Tee (2005).

Values of C_f are calculated from typical ice-crystal habits shown by Takana and Liou (1995) are reproduced in Fig. 3. Their results are used because they provide both G and the true volume V for these ice crystals making it possible to calculate C_f. The possibility of varying the shown dimensions of the crystals in Fig. 3 can result in many calculations. Here we chose a wide selection of dimensions that likely still does not fully represent the broad geometric complexity of small ambient ice crystals. The result of the calculations are shown in Fig. 4.; equations for the curves in Fig. 4 are found in Gerber and DeMott (2014).

4. COMPARISON OF MEASURED AND REFERENCE VALUES OF Re

Ten experiments of the18 experiments run in the DCC provided usable data; and for the usable experiments a total of 18 ~60-s intervals were studied in detail where ice crystal images were manually evaluated using the video microscope, and reference values were calculated for LWC and Re. The upper plot of Figure 5 shows the uncorrected FSSP and PVM measurements of Re (FSSPRe, PVMRe) for each interval compared to the reference Re (TOTREFF). The lower plot shows the measured values after application of the correction factor C_f .

The difference between the two plots in Fig. 5 can be explained as follows: Whereas, the PVM Re values agree quite well with the reference Re in the upper plot while the FSSP results overestimate Re as expected, the PVM results are fortuitous because two other factors caused the PVM to underestimate Re: The PVM was observed to evaporate ice crystals in the DCC due to heat release from the PVM, and it's smaller upper size response limit in comparison to the FSSP caused larger crystals to be missed. The lower plot shows good agreement with the FSSP Re after C_f is applied, while the PVM Re shows significant underestimates except for periods where the crystals were within its size response range and where ice-crystal evaporation was reduced.

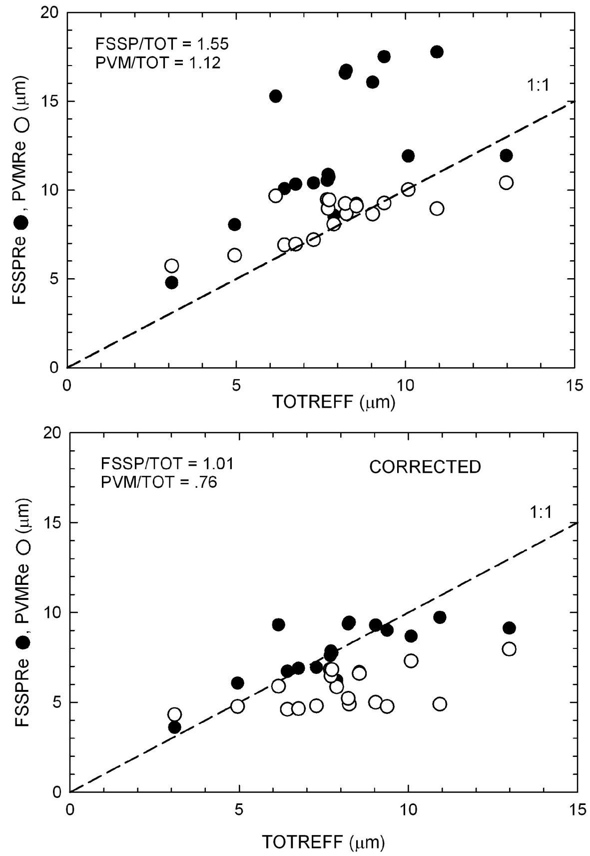

Fig. 5 - Mean effective radius (Re) in ice clouds (upper panel) measured by the FSSP and PVM in each in analysis interval of the 10 DCC experiments, and the same measurements adjusted with the volume correction factor (lower panel) as a function of the reference Re given by TOTREFF.

5. CONCLUSIONS

o It is possible to correct overestimates of IWC and Re made by forward-scatter probes such as the FSSP and PVM for randomly-oriented single ice crystals of typical hexagonal shape by applying a calculated ice volume correction factor C_f .

o Ice crystal measurements in the CSU dynamic cloud chamber (DCC) show that both the FSSP and PVM behave approximately as "laser-diffraction instruments" where light scattered by ice crystals would be dominated by diffracted light. A more precise conclusion is limited by resolution of the measurements.

o Measurements of ice crystals with the PVM located in the DCC proved difficult primarily because of ice-crystal evaporation by heat released from the probe, and also because of the probe's limited response to larger crystals.

o The application of the present calculations of the correction factor C_f for small ice crystals to forward-scatter probes used during aircraft measurements in ice clouds depends on the assumption that small ambient ice crystals are randomly oriented during the measurements. Such orientation for small crystals under those conditions is not well established.

Acknowledgments

The present analysis was supported by NASA Goddard Grant NNX11AB67G. Thanks are also due David Rogers. who participated in the original study.

6. REFERENCES

Baumgardner, D., et al., 2011: Airborne instruments to measure atmospheric aerosol particles, clouds and radiation. A cook's tour of mature and emerging technology. *Atmos. Res.*, 9, 10-29.

DeMott, P.J., 1988: Comparison of the behavior of AgI-type ice nucleating aerosols in the laboratory. *J. Weather Mod.,* 20, 444-450.

DeMott, P.J., 1990: Exploratory studies of ice nucleation by soot aerosols. *J. Appl. Meteor.*, 29, 1072-1079.

DeMott, P.J., and D.C. Rogers, 1990: Freezing nucleation rates of dilute solution droplets measured between -30C and -40C in laboratory simulations of natural clouds. *J. Atmos. Sci., 47*, 1056-1064

Gerber,H., P.J. DeMott, and D.C. Rogers, 1995: Laboratory investigation of direct measurement of ice water content, ice surface area, and effective radius of ice crystals using a laser-diffraction instrument. *Final Report (NAS-14261*, NASA Ames Research Center, pp. 142. (http://ntrs.nasa.gov/archive/nasa/casi.ntrs.gov/-20000023203/2000022171.pdf).

Gerber, H., and P.J. DeMott, 2014: Response of the FSSP-100 and PVM-100A to small ice crystals. J. Atm. Oceanic. Technol., in print.

Heymsfield, A.J., and L.M. Miloshevich, 2003: Parameterization for the cross-sectional area and extinction of cirrus and stratiform ice cloud particles. *J. Atmos. Sci.*, 60, 936-956.

Heymsfield, A. J., C. Schmitt, A. Bansemer, and C.H. Twohy, 2010: Improved representation of ice particle masses based on observations in natural clouds. *J. Atmos. Sci.*, 67, 3303-3318.

Korolev, A.V., E.F. Emery, J.W. Strapp, S.G. Cober.G.A. Isaac, M. Wasey, and D. Marcotte, 2011: Small ice particles in tropospheric clouds: Fact of artifact? *Bull. Amer. Meteor. Soc.* 92, 967-973.

Korolev, A.V., E. Emery, and K. Creelman, 2013: Modification and tests of particle probe tips to mitigate effects of ice shattering. *J. Atmos. Oceanic Technol.*, doi:10.1175/JTECH-D-12-00142.1.

Redder, C.R., and N. Fukuta, 1989: Empirical equations of ice crystal growth microphysics for modeling and analysis. I. Mass and dimensions. *Atm. Res.*, 24, 247-272.

Tee, G.J., 2005: Surface area and capacity of ellipsoids in n dimensions. New Zealand J. Of Math. 34, 165-198. (http://www.citr.aukland.ac.nz/techreports/2004/CITR-TR-139.pdf).

Takano, Y., and K.N. Liou, 1989: Solar radiative transfer in cirrus clouds. Part I: Single-scattering and optical properties of hexagonal ice crystals. *J. Atmos. Sci.*, 46, 3-19.

Van De Hulst, H.C., 1962: *Light Scattering By Small Particles*. John Wiley & Sons, pp. 470.

Wendisch M., and J.-L. Brenguier, 2013: *Airborne Measurements for Environmental Research - Methods and Instruments*. Eds. M. Wendisch and J.-L Brenguier, doi:10.1002/9783527653218, pp. 791.